Ultrasound in Med. & Biol., Vol. 48, No. 10, pp. 2040–2051, 2022

0301-5629/$ - see front matter

https://doi.org/10.1016/j.ultrasmedbio.2022.05.028

● *Original Contribution*

EFFECTS OF OSMOLARITY ON ULTRASOUND-INDUCED MEMBRANE DEPOLARIZATION IN ISOLATED CRAYFISH MOTOR AXON

FEIYUAN YU,* WOLFGANG S. MÜLLER,† GÖSTA EHNHOLM,‡ YOSHIO OKADA,† and JEN-WEI LIN*

* Department of Biology, Boston University, Boston, Massachusetts, USA; † Department of Neuroscience and Biomedical Engineering, Aalto University, Aalto, Finland; and ‡ Division of Newborn Medicine, Department of Pediatrics, Boston Children's Hospital and Harvard Medical School, Boston, Massachusetts, USA

(*Received* 2 *December* 2021; *revised* 17 *May* 2022; *in final form* 19 *May* 2022)

Abstract—We have previously identified a novel non-selective membrane conductance (g_{US}) opened by focused ultrasound (FUS) in crayfish motor axons. In the work described here, we studied g_{US} properties further by comparing FUS-evoked depolarization (FUSD) in control and hypotonic saline with 75% of control osmolarity. The FUS was a train of 20 FUS bursts (2.1 MHz and 50 μs per burst) delivered at 1 kHz. The amplitude, onset latency, frequency of occurrence and duration of FUSD were compared in a 15-min time window before and after switching to hypotonic saline. Significant increases were observed for amplitude ($p < 0.001$) and frequency of occurrence ($p < 0.01$) while the onset latency exhibited a significant decrease ($p < 0.001$). FUSD duration did not significantly differ. These results support predictions based on our hypothesis that g_{US} is mediated by opening of nanopores in the lipid bilayer and that stretching of axonal membrane caused by swelling at low osmolarity should increase the probability of nanopore formation under FUS. The FUSD parameters, in addition, exhibited time-dependent trends when the window of observation was expanded to 45 min in each saline. The statistical significance of amplitude and duration differed between 15- and 45-min time windows, indicating the presence of adaptive responses of axonal membrane to osmotic manipulation. (E-mail: jenweilin@bu.edu) © 2022 Published by Elsevier Inc. on behalf of World Federation for Ultrasound in Medicine & Biology.

Key Words: **Focused ultrasound, Neuromodulation, Neurostimulation, Crayfish motor axon, Osmolarity, Membrane conductance, Lipid bilayer, Biophysical mechanism of ultrasound.**

INTRODUCTION

Focused ultrasound (FUS) is increasingly recognized as a promising modality for non-invasive neural modulation because of its ability to stimulate deep brain areas with fine spatial resolutions and power levels within the U.S. Food and Drug Administration (FDA) safety limits (Tufail et al. 2010; Tyler et al. 2008, 2010). In comparison to transcranial magnetic stimulations or transcranial electrical stimulations, FUS has the advantage of deeper penetration while maintaining a fine, millimeter resolution (Clement and Hynynen 2002).

The mechanisms underlying FUS-based neuromodulation are being actively studied to help advance the application of FUS approaches for brain activation (Heimburg 2010; Naor et al. 2016; Blackmore et al. 2019; Feng et al. 2019; Zhang et al. 2021). While mechanical impacts generated by US on target neurons could be mediated through multiple physical processes, FUS-generated mechanical disturbance ultimately may influence neuronal activity by modulating mechanosensitive domains of voltage-gated channels (Morris and Juranka 2007; Kubanek et al. 2016) or mechanosensitive channels (Kubanek et al. 2016, 2018; Wu et al. 2017). FUS may alter membrane excitability by stretching and compressing the lipid bilayer and thus generating capacitive currents (Prieto et al. 2013).

In our previous study using single motor axons (Lin et al. 2019), we found FUS-induced depolarization (FUSD) could best be explained by a non-selective conductance (g_{US}). The membrane depolarization induced by g_{US} could reach a maximum of 50 mV in amplitude with a long duration (2.1 s on average and 200 s at maximum) and a relatively fast onset time (mean = 3.4 ms). The reversal potential was estimated to be −8.4 mV, suggesting that the conductance was non-selective to ions. Potential contribution of voltage-gated channels to FUSD was ruled out because this depolarization was recorded in the presence of blockers of voltage-gated

Address correspondence to: Jen-Wei Lin, Department of Biology, Boston University, 5 Cummington Mall, Boston, MA 02215 USA
E-mail: jenweilin@bu.edu

channels. Mechanosensitive channels or capacitive current, caused by membrane stretching or compression, were also consider unlikely because FUSD persisted for seconds, long after millisecond-long FUS tone bursts had ended. The combination of these characteristics and the fact that g_{US} was non-selective led us to propose that nanopores in axonal membrane, that is, lipid ion channels (Heimburg et al. 2010), should be the most likely mechanism underlying g_{US}.

In this study we characterized g_{US} further in the crayfish motor axons. Molecular dynamic simulations have suggested that electroporation and stretch of membrane lipid bilayers could increase the probability of formation of hydrophilic pores that could be semi-stable (Tieleman et al. 2003; Hu et al. 2005). In the work described here, we used hypotonic saline to induce cell swelling and increase the lateral tension of axonal membrane, and we examined whether the occurrences as well as other characteristics of FUSD may be enhanced as predicted by the nanopore hypothesis.

METHODS

Preparation and solutions

Crayfish, *Procambarus clarkii*, were purchased from Niles Biological Supplies (Sacramento, CA, USA). Small animals of both sexes, 5−7 cm head to tail, were maintained in tap water at room temperature (22˚C). All experiments were performed at the same temperature. The first walking leg was removed by autotomy and fixed with cyanoacrylate (KG86648R, Elmer's Products, Westerville, OH, USA) to a 60-mm-diameter plastic Petri dish (No. 430589, Corning, NY, USA). The opener axon−muscle preparation was dissected in saline. Recordings from both excitatory and inhibitory axons were polled for statistical analysis in this study because previous imaging and electrophysiological studies had reported that the two axons are similar in their basic structural and physiological properties (Wright et al. 1996; Vyshedskiy and Lin 1997). The bathing medium was a physiological saline with the following composition (in mM): 195 NaCl, 5.4 KCl, 13.5 $CaCl_2$, 2.6 $MgCl_2$ and 10 Hepes, titrated to pH 7.4 with NaOH. The saline was circulated by a peristaltic pump at the rate of 1.5 mL/min. Three pharmacological stock solutions were prepared: (i) 4-aminopyridine (4-AP, 1 M), which blocks the dominant low-threshold potassium channels (Lin 2012), was dissolved in distilled water; (ii) tetrodotoxin (TTX, 1 mM), which blocks sodium channels, was dissolved in distilled water; and (3) ZD7288 (50 mM), which blocks hyperpolarization-activated cation channels, was dissolved in dimethyl sulfoxide (DMSO). The stock solutions were stored at −20C˚ and added to the saline directly after each solution reached room temperature. ZD7288 was purchased from TOCRIS Bioscience (Bristol, UK). All other chemicals were from Sigma-Aldrich (Burlington, MA, USA). The perfusion inlet was positioned within 5 mm of, and aimed at, the preparation such that the change of solution at the axons was nearly instantaneous when channel blockers or hypotonic saline reached the recording dish (Lin et al. 2019).

Reduction in osmolarity was achieved in two ways. First, the circulating saline was diluted with distilled water to 75% of this original osmolarity. As the dilution reduced concentrations of ions, we also use a second saline preparation to mitigate this confound. In the second saline preparation, NaCl in control saline was reduced from 195 to 150 mM, which is ∼75% of total NaCl, and 90 mM sucrose or mannitol was added to restore the osmolarity. The reduction in osmolarity was achieved by the same saline in the absence of sucrose or mannitol. Sucrose-substituted experiments were tested in eight preparations, and mannitol in three. The osmolarity measured, using Osmometer 3D3 (Advanced Instruments, Norwood, MA, USA) and in quadruplicate, from these solutions were as follows (in mOsm): control saline (429 ± 5.4), control saline diluted with distilled water (326 ± 1.6), mannitol-substituted saline (444 ± 7.5), sucrose-substituted saline (455 ± 10.8) and sugar-free saline (350 ± 4.7). Percentage reduction of osmolarity of the three saline variants ranged from 75% to 78%.

Experimental configuration

Experimental configurations have been detailed in a previous study (Lin et al. 2019) and are illustrated in Figure 1 for visualization. Briefly, the two electrodes for two electrode current clamps approached axons from the same distal-to-proximal direction, while the FUS transducer approached the preparation from the opposite direction (Fig. 1A). Recordings provided in this article were obtained mainly from the secondary branches (Fig. 1B, *red*). Axon penetrations were performed under a 40 × /0.80w water immersion lens (LUMPlanFl/lR, Olympus, Tokyo, Japan), which was then removed to make room for the FUS transducer. The transducer was angled at 45˚, and microelectrodes at 28˚, to the horizontal plane (Fig. 1A). The FUS transducer was brought as close to the preparation as possible, with the lower edge of the FUS transducer cone ∼1 mm from the bottom of the recording dish. The distance was estimated visually in most experiments, but it had been verified by digital readouts of a motorized manipulator (MP-285, Sutter Instrument, Novato, CA, USA). For its optimal localization, the transducer was moved horizontally until the amplitude of a hyperpolarization transient was maximal (Lin et al. 2019). The localization coincided with having

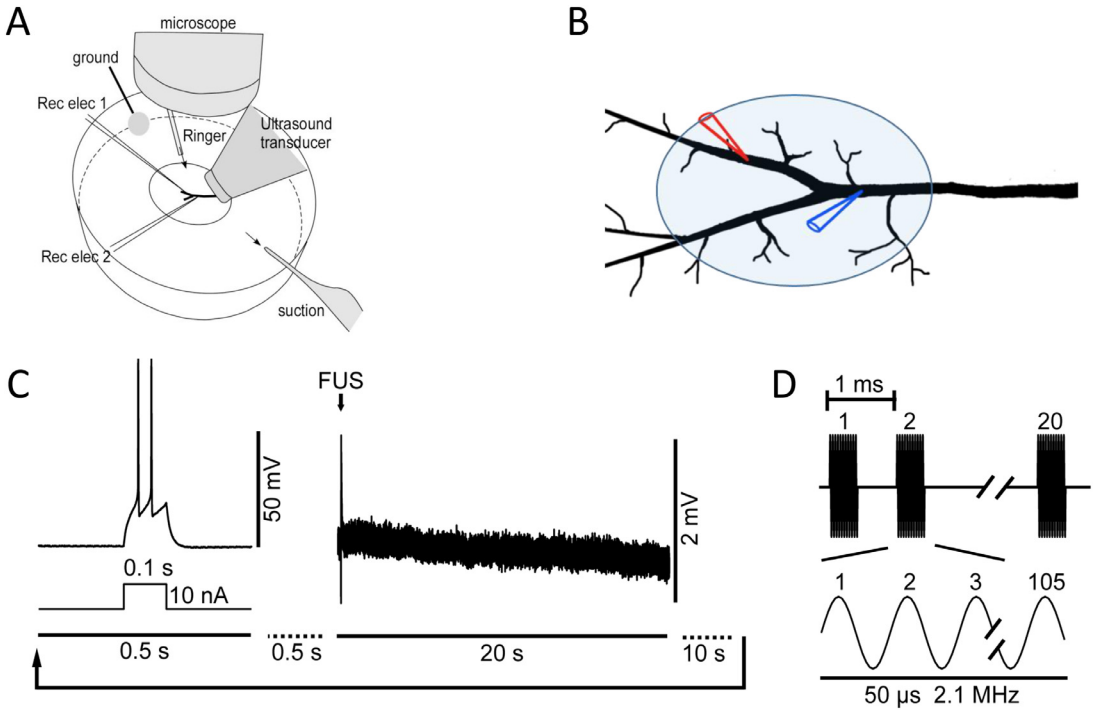

Fig. 1. Experimental configurations and protocols. (A) Crayfish opener neuromuscular preparation with two recording electrodes (Rec elec), 1 and 2, respectively, together with ultrasound transducer placements. (B) Detailed two-electrode current clamp configuration, with one electrode at the primary branch (*blue*) and the second electrode at the secondary branch (*red*). Also shown is the approximate footprint of a typical US focal area when the transducer is angled at 45° (*shaded ellipse*). The dimensions of the axon are equivalent to a preparation dissected from a large animal 6 cm in length head to tail. The US focal area coverage, relative to axonal arborization, is likely to be more extensive in some smaller animals used in this study. (C) Timeline of a typical experiment. A 10-nA current injection was alternated with US tone burst. The time gap between the current step and FUS tone burst was 0.5 s. FUSD was recorded as 20-s-long traces. The time gap between the FUS test trace and the next 10-nA current step was 10 s. (D) The FUS tone burst consists of 20 pulses of 50-μs tone bursts (2.1 MHz) delivered at 1 kHz. FUS = focused ultrasound; FUSD = FUS-evoked depolarization.

most of the axonal arborization enclosed within the diameter of the US focal point (~1 × 1.4 mm) (Lin et al. 2019). This procedure ensured that FUS-induced responses could be triggered by the lowest possible intensity.

FUS-induced responses reported here were evoked by a train of 20 FUS pulses (2.1 MHz), each pulse lasting 50 μs (Fig. 1D), delivered at 1 kHz. In other words, each pulse train lasted 20 ms with a duty cycle of 5%. A typical experimental cycle included a test current step to trigger action potentials (Aps), to monitor axonal excitability (Fig. 1C, left), followed by a trial testing effect of the FUS tone burst (Fig. 1C, right). Responses evoked by a single train of 20 FUS pulses were recorded in a trace lasting 20 s. There was then a 10-s gap after the end of the US monitor traces and before the next test current was injected (Fig. 1C). Both APs evoked by current steps (500 ms in recording duration) and FUS-evoked responses (20 s in recording duration) were sampled at the rate of 50 KHz.

FUS transducer

The active element of the transducer was a spherical piezo cup from Steminc Piezo (SMSF20C30F21, Steiner & Martins, Davenport, FL, USA). The piezo cup was driven by a mini-circuit amplifier (LZY-22+, Mini-Circuits, Brooklyn, NY, USA) which in turn was modulated by a function generator (DG1022, Rigol, Beijing, China). The cup had a diameter of 20 mm and spherical radius of 30 mm, which was also the focal length of the conical ultrasound beam from the cup. Rexolite (C-Lec Plastics, Philadelphia, PA, USA), a cross-linked polystyrene with low ultrasound absorption (impedance = 2.48 MRayl) and a low reflection coefficient from soft tissues, was machined into a conical shape with the large end fitting exactly to the inside of the piezo cup. FUS sound waves passed through the cone and reached the tip of the cone, which was machined down to a concave sphere to increase the focus and FUS power. The tip pulled the original focal point closer to the transducer when it was submerged in saline. The Rexolite-to-saline interface

formed a lens that made the focal spot smaller. As characterized previously, a focused FUS beam with a circular cross section of 1-mm diameter and at a 45° angle should project an elliptic focal image on the preparation with minor and major axes of 1 and 1.44 mm, respectively (Fig. 1B). The lowest possible FUS pressure capable of triggering FUSD, in ~10% of the trials, was chosen for each preparation. Based on calibrations of the same transducer reported previously (Lin et al. 2019), the pressure typically ranged from 0.1 to 0.3 MPa, which was well below the maximal pressure (0.75 MPa) the transducer was capable of delivering. Taking into account Rexolite impedance and duty cycle (1-ms total burst duration/20 s), the intensity of the spatial peak temporal average (I_{SPTA}) of FUS at the focal point should be 0.94 mW/cm^2. The intensity is lower than the FDA safety limit for applied temporal average energy level of <720 mW/cm^2 (Miller 2008).

Electrophysiology

Two DC amplifiers (IE-210, Warner Instruments, Hamden, CT, USA) were used to perform two-electrode current clamp. Voltage signals were low pass filtered at a cutoff frequency of 5 kHz and digitized at 50 kHz. Data were digitally sampled with a NI 6251 board (National Instruments, Austin, TX, USA) and analyzed with IGOR (Wavemetrics, Lake Oswego, OR, USA). Microelectrodes were filled with 500 mM KCl and had a resistance of 40−60 MΩ. The typical resting membrane potential (V_m) was approximately −70 mV.

Each preparation represents a recording session from a motor axon dissected from an animal. A recording session typically lasted 2−4 h. The preparations can be grouped into two subsets based on pharmacological conditions. Group 1 (n = 5) FUS-evoked responses were recorded without channel blockers. Group 2 (n = 3) preparations were treated with TTX (1 μM), 4-AP (200 μM) and ZD7288 (50 μM). While three of the eight preparations used in statistical analysis were studied in the presence of channel blockers, most FUSDs were subthreshold to AP initiation and were minimally affected by these drugs. Therefore, parameters characterizing FUSDs from both sets of preparations, with and without blockers, were pooled for data analysis.

Data analysis

Statistical results presented in graphs are expressed as averages and standard deviations (SD) or standard errors of means (SEM). Statistical significance was determined with a paired Student's *t*-test. Estimates of the membrane time constant used the single-exponential curve fitting routine in IGOR.

RESULTS

Basic characteristics of action potentials and FUSD in hypotonic saline

Focused ultrasound depolarization was evoked by applying a brief train of 20 US pulses (2.1 MHz and 50 μs induration) delivered at 1 kHz. FUSD occurred stochastically as reported previously. The depolarizations were suprathreshold for eliciting action potentials (APs) in some trials (Fig. 2A) while subthreshold in others (Fig. 2B). In the examples provided in Figure 2A and B, FUSD traces recorded in hypotonic saline (*red*) exhibited larger amplitudes and shorter delays compared with those recorded in control saline (*black*). Insets in (A) and (B) depict the same traces with a faster time scale, and FUS delivery periods are indicated by the *black bars*. Subthreshold FUSDs typically exhibited a rapid rising phase with a prolonged decay (Fig. 2B). The stability of the electrode recording was monitored during the experiment by a 10-nA current step delivered between FUS trials (Figs. 1C and 2C). *Arrows* in Figure 2D, using the same trace as the black one in Figure 2C, identify the time window used to determine the membrane time constant. Figure 2E and 2F illustrate the timelines of four parameters of the FUSD and AP measured during a typical experimental session over a 90-min period: (i) amplitudes of FUSD (Fig. 2E, left axis), (ii) AP amplitude evoked by current steps (Fig. 2E, right axis), (iii) resting membrane potential (Fig. 2F, left axis) and (iv) membrane time constant (Fig. 2F, right axis). (*Red symbols* in Fig. 2E identify the trials from which traces in A, B and C, with corresponding symbols, were obtained.) The time during the control saline is represented by the white background, and that during the hypotonic saline condition, by the pink background. Because of the stochastic nature of the FUS-induced responses, the density of data points corresponding to FUSD (Fig. 2E, *filled circles*) was not as high as that evoked by step current injections (Fig. 2F, *gray triangles*). FUSD exhibited slightly higher incidences of occurrence after transitioning into hypotonic saline, while AP amplitudes evoked by current steps did not exhibit appreciable change. There was a slight drift in resting membrane potential (RMP), but lowering osmolarity did not disrupt the continuous drift in RMP (Fig. 2F, *filled circles*). Although time constants appeared to decline after switching to hypotonic saline in this preparation, this change was not a consistent finding. The RMP was measured during the 20-ms baseline before the current step or FUS was delivered in each digitized trace. In each preparation the RMP was averaged across all the trials during a 15-min time window before and after lowering osmolarity. Averaged RMP values from eight preparations were −68.4 ± 3.4 mV before and −68.0 ± 5.7 mV after switching to hypotonic saline.

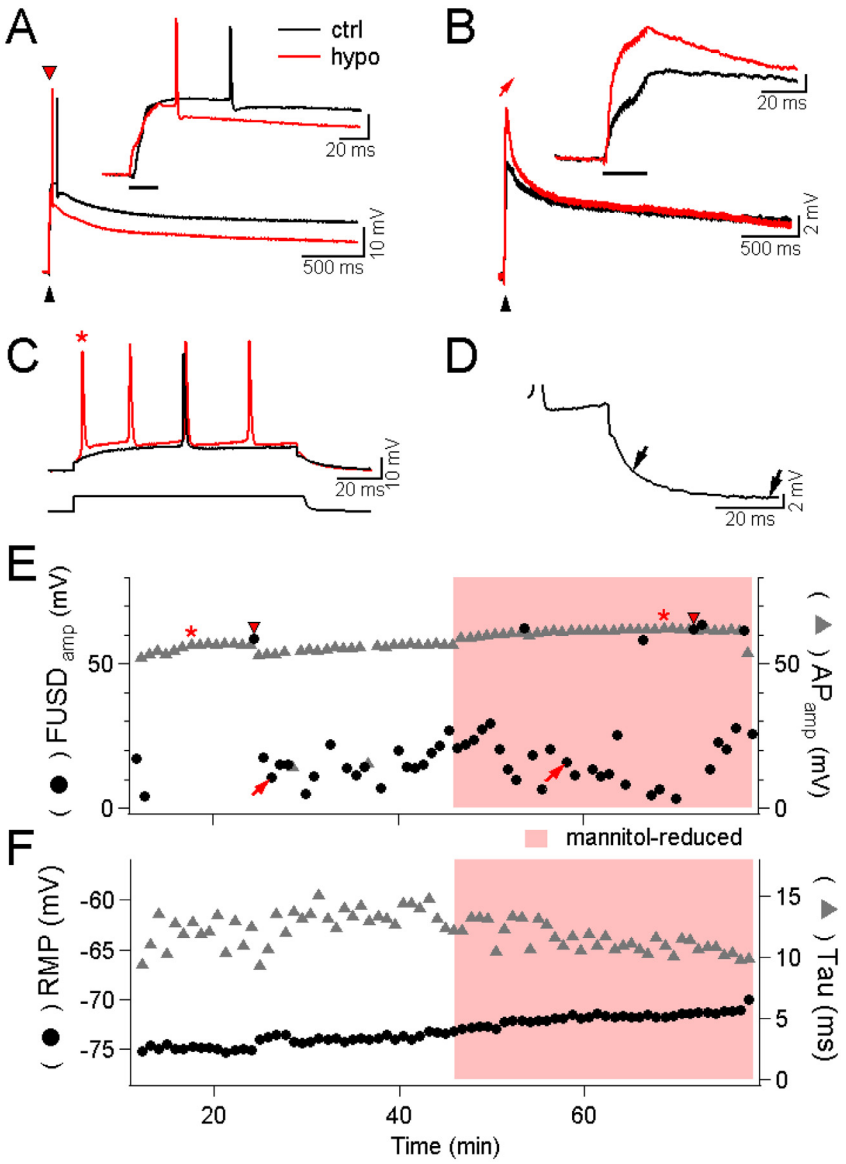

Fig. 2. Effects of hypotonic saline on passive and active membrane properties in crayfish axons. (A) Suprathreshold responses evoked by FUS tone burst. Inset: initial part of US evoked responses displayed in expanded time scale. The recordings were obtained from the data points marked by *inverted red triangles* in (E). (B) Subthreshold responses evoked by the same US tone bursts. The traces were obtained from the time point marked by *red arrows* in (E). In (A) and (B), the timing of US delivery is marked by the *arrowhead* in the main graphs and *horizontal bar* in the insets. (C) Examples of AP evoked by 10-nA steps recorded in control and hypotonic saline. The recordings were obtained from the time points marked by *asterisks* in (E). (D) *Arrows* identify the time window during which single exponential fits were applied for time constant estimates. This trace is identical to the black trace in (C). (E) Timeline plots of the amplitudes of FUSD ($FUSD_{amp}$) and action potential (AP_{amp}) in control and hypotonic saline (*shaded area*). Switching to hypotonic saline induced minimal changes in both parameters. (F) Timeline plots of resting membrane potential (RMP) and membrane time constant (Tau). (E) and (F) share the same time axes. Low osmolarity in this experiment was achieved by removing 90 mM mannitol from a "control" saline in which 45 mM NaCl had been replaced by 90 mM mannitol. FUS = focused ultrasound; FUSD = FUS-evoked depolarization.

This change represents a continuous drift in DC level not related to osmolarity because there was no stepwise change in this parameter associated with the reduction of osmolarity. The time constant of the membrane, measured using the same 15-min time windows as those of RMP, remained the same when the osmolarity was decreased: 10.2 ± 1.13 ms before and 10.2 ± 1.11 ms after (n=7) switching to hypotonic saline, respectively. (The sample size for the time constant was 7 because 10-nA test current steps were not used in one

preparation.) Overall, these results indicate that the hypotonic solution did not noticeably alter the passive or active membrane properties of the axon.

Effects of hypotonic saline on properties of FUSD

Figure 3 illustrates the analysis of four parameters used to characterized FUSD. Figure 3A illustrates how amplitude, duration and delay of the FUSD were defined. Duration was defined as the width of the subthreshold depolarization at 50% of maximal amplitude (Dur_{50}). Delay (Del) of FUSD was defined as the time between the onset of FUS pulse train to the time when FUSD crossed a threshold of 2 mV (Fig. 3A, inset). The time axis in Figure 3B–E is bracketed such that the equal times (45 min) are displayed before and after switching to low osmolarity as in Figure 2. Hypotonic saline enhanced the amplitude (Fig. 3B) and frequency of occurrence of FUSD (Fig. 3D). The FUSD became

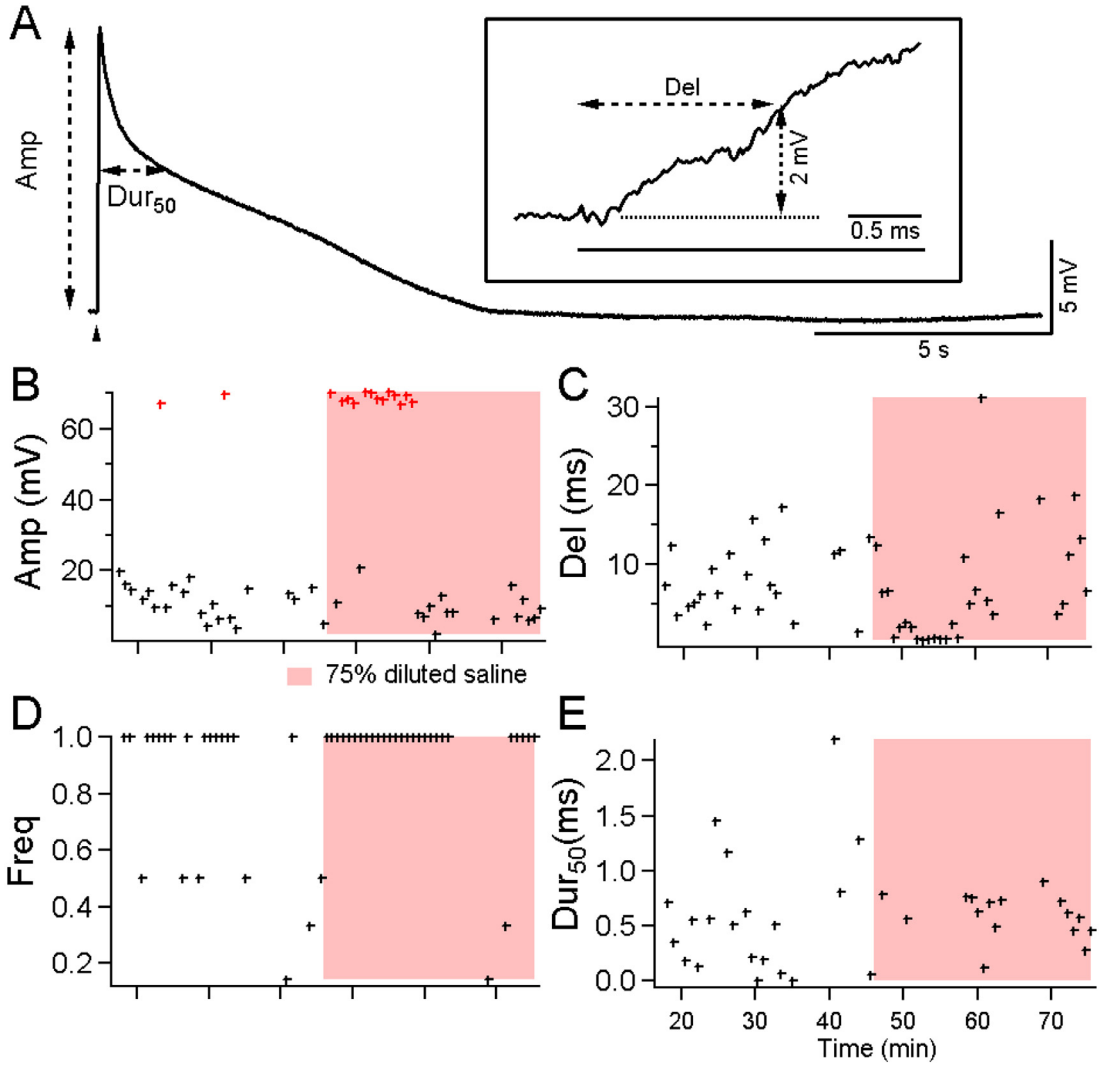

Fig. 3. Quantitative analysis of US-evoked physiological parameters measured in control and low-osmotic saline. (A) Illustration of measurements of amplitude, 50% duration and delay of ultrasound-induced responses (inset). The *arrowhead* and the *horizontal bar in the inset* indicate the timing of US tone burst delivery. (B) Timeline of the amplitude of focused ultrasound–evoked depolarization. *Red crosses* identify suprathreshold responses. (C) Timeline of the delay of ultrasound-induced responses. (D) Normalized frequency of occurrence of ultrasound-induced responses. The frequency of 1 means a ultrasound tone burst successfully evoked responses in consecutive trials. (E) Timeline of half-maximal duration of subthreshold response. The data points in (E) do not fully correspond to those in (B), (C) and (D) because the durations were not measured in trials where the US evoked action potentials. The numbers of data points in (B), (C) and (D) for control and hypotonic saline were 22 and 29, respectively. The numbers of data points in (E) were 20 and 16 for control and hypotonic saline, respectively.

suprathreshold for eliciting AP in most of the trials during the first 15 min after switching from normal to hypo-osmolar saline (Fig. 3B, *red crosses*). The delay of FUSD was consistently reduced, immediately after switching the solution to 75% osmolarity (Fig. 3C). The instantaneous frequency of occurrence of FUSD for each FUSD was defined as 1 when there was a FUSD on the preceding trial. The frequency was 0.5 and 0.3 when the previously detected FUSD was observed at two or three trials before the FUSD in question. As illustrated in Figure 3D, FUS succeeded in eliciting a depolarization in every trial, with a frequency of one, after switching to hypotonic saline in this preparation. The depolarization duration Dur_{50} varied considerably in the control and hypotonic saline and this parameter did not exhibit any noticeable change when the osmolarity was lowered. (Note that the number of data points in Figure 3E is lower than the numbers in panels B, C and D because Dur_{50} was not measured on trials that evoked APs.)

To evaluate the statistical significance of changes induced by hypotonic saline, the parameters shown in Figure 3 from eight preparations were normalized first before being combined. Specifically, in each preparation, values measured from every detectable FUSD trial in control saline were averaged. The average was then used to scale all the trials, including those in hypotonic saline, such that the average value for all the control trials was one. The normalized data from all eight preparations were then merged into a single composite timeline.

Figure 4A illustrates the composite timeline of the amplitude of subthreshold FUSD, in 5-min time blocks, over a period of 90 min, with error bars representing standard errors of the mean. The amplitude timeline exhibits an abrupt jump when hypotonic saline was introduced, despite a declining trend during control period (Fig. 4A). The FUSD delay exhibited a step decrease on switching to hypotonic saline (Fig. 4B). The instantaneous frequency of occurrence of FUSD increased after the switch (Fig. 4C). The duration (Dur_{50}) did not significantly change immediately after switching to hypotonic saline.

These qualitative trends were analyzed statistically by comparing the parameters during the 15-min periods (three data blocks) before and after the switch to the hypotonic medium. The normalized subthreshold amplitude increased from 0.71 ± 0.07 to 1.28 ± 0.12 (*t*-test, $p = 4 \times 10^{-5}$) after lowering the osmolarity. The delay of FUSD was significantly shorter after the saline switch, from 1.13 ± 0.18 to 0.44 ± 0.05 (*t*-test, $p = 1.8 \times 10^{-4}$). The frequency of occurrence increased from 0.97 ± 0.03 to 1.09 ± 0.02 (*t*-test, $p = 1.4 \times 10^{-3}$). There was no significant change in Dur_{50} (0.72 ± 0.21 vs. 0.89 ± 0.13 (*t*-test, $p = 0.28$) during the 15-min time window before and after lowering osmolarity.

Although the changes in these parameters were clearly significant during the 15-min period after the switch compared with the same period just before the switch, the pattern of data was more complex over the entire 45-min period before and after the switch. Statistical analysis was carried out over the entire 45-min period before and after the switch (Table 1). Amplitude averaged over 45 min did not change significantly in the 75% hypotonic saline compared with the control. The average delay over the 45 min remained significantly lower as for the 15-min time window. The significant increase in frequency of FUSD seen during the first 15-min period remained during the 45 min period**.** Although Dur_{50} did not significantly decrease with the first 15-min time window, the decrease over the entire 45 min was significant. The RMP and membrane time constant, which are two basic indicators of the stability of passive membrane properties, did not exhibit any significant change as the preparations were switched in and out of hypotonic saline (Table 1).

DISCUSSION

We examined the effect of lowering osmolarity on FUSD in crayfish motor axons. Lowering osmolarity to 75% of the control level did not change passive and active properties of the axon but altered the characteristics of FUSD produced by FUS tone bursts. Statistically significant changes in FUSD parameters were observed when comparing recordings from a 15-min time window before and after switching to hypotonic saline. Specifically, the amplitude and frequency of the FUSD occurrences increased, while the delay of FUSD decreased in hypotonic saline. The duration of the FUSD, however, did not statistically differ in the 15-min time window. These changes are consistent predictions based on the nanopore hypothesis. Expanding the time window of comparison to 45 min changed the status of statistical significance of FUSD amplitude, from significant to insignificant, and that of duration, from insignificant to significant, while the statistical significance of delay and frequency of occurrence was unaffected by the time windows selected for the comparison.

Using the crayfish neuromuscular junction as a model system to study FUS neuromodulation

In the study described here, the motor axons of the crayfish opener neuromuscular junction were used to investigate US-mediated neuromodulation under the condition of low osmolarity. The crayfish nerve–muscle preparation is one of the classic model systems that has contributed to the understanding of basic neurophysiological mechanisms of membrane excitability and synaptic transmission (Atwood 2008; Lin 2013). The

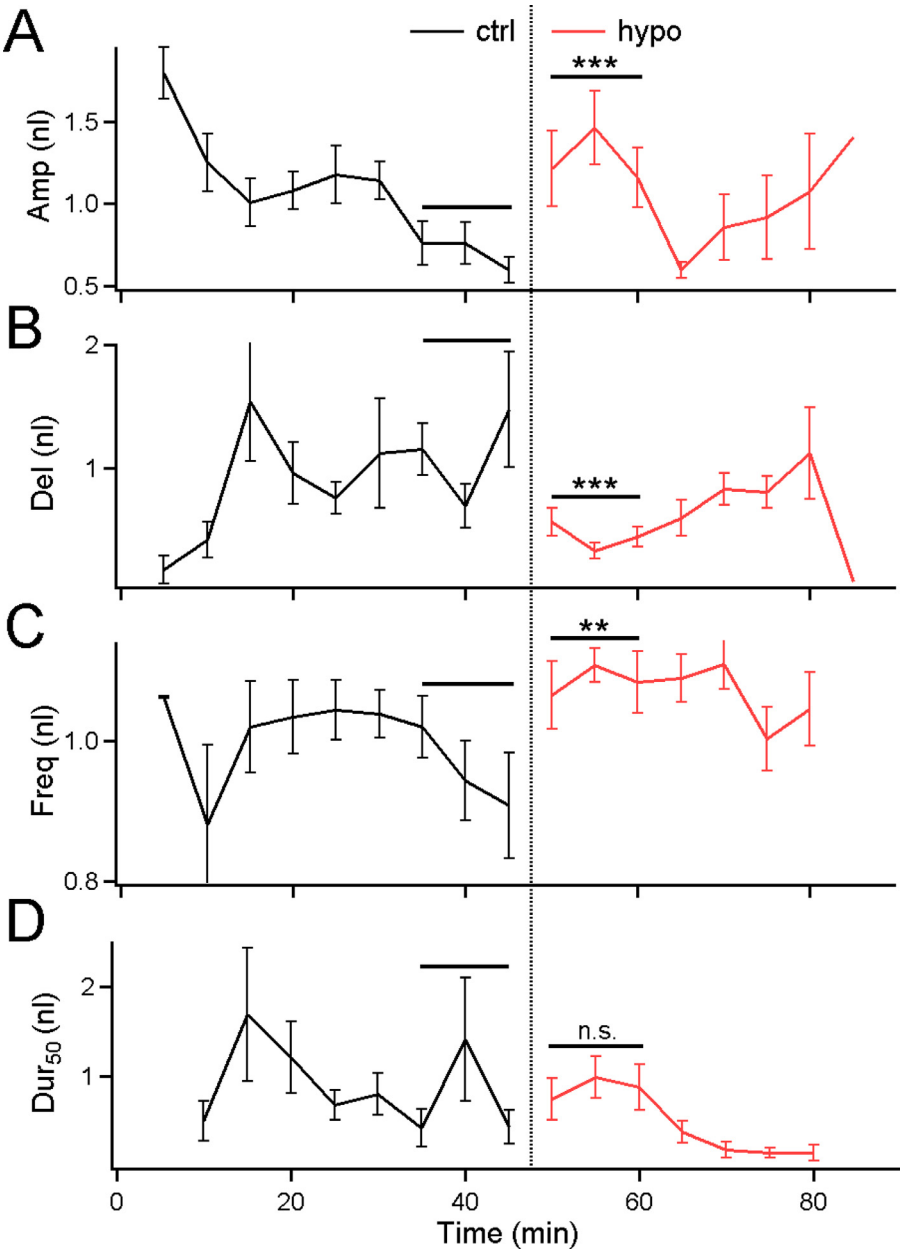

Fig. 4. Compilation of changes in ultrasound-induced depolarizations as osmolarity was lowered. Average and standard error of means of normalized amplitude (A), delay (B), frequency of occurrence (C) and Dur_{50} (D) plotted in 5-min blocks. The transition from control (*black*) to hypotonic (*red*) saline occurred at 45 min. A set of eight preparations were used for statistical analysis in this report. For the preparation of hypotonic saline, one of the eight preparations used sucrose substitution, two used mannitol substitution and the remaining five used distilled water dilution. The sample size for each data point ranged from 4 to 12. For (A) and (D), the total numbers of FUSD events were 73 in control saline and 100 in hypotonic saline. For (B) and (C), the sample sizes were 82 in control and 105 in hypotonic saline. Smaller sample sizes in (A) and (D) were due to exclusion of trials in which FUSD was suprathreshold and evoked action potentials. FUSD = FUS-evoked depolarization.

simplicity and hardiness of this preparation have been exploited for the initial implementations of new technologies such as calcium uncaging and calcium imaging (Delaney et al. 1989; Mulkey and Zucker 1993). This preparation has continued to prove useful; it has recently been used to explore biomedical applications of new technologies, such as ultrasound and infrared laser, in neuromodulation (Lin et al. 2019; Zhu et al. 2019).

Table 1. Statistical analysis of the physiological parameters of ultrasound-induced responses in control and hypotonic saline

	Amplitude* (mV)	Frequency† (nl)	Delay (ms)	Dur_{50} (ms)	RMP (mV)	Time constant (ms)
Control (n = 8)	18.5 ± 3.3	0.77 ± 0.11	11.9 ± 4.9	598 ± 154	68.4 ± 3.4	10.2 ± 1.13
p Value	0.447	**0.025**‡	**0.034**	**0.03**	0.437	0.483
75% Hypotonic	19.0 ± 4.0	0.85 ± 0.09	8.0 ± 3.2	341 ± 97	68.0 ± 5.7	10.2 ± 1.11
p Value	0.268	0.447	0.348	0.146	0.290	0.086
Recovery	21.5 ± 3.5	0.87 ± 0.05	5.5 ± 1.6	577 ± 210	67.7 ± 3.9	8.21 ± 0.85

RMP = resting membrane potential.

Detectable focused ultrasound−evoked depolarization used for averaging were collected over a period of 45 min immediately before and after switching from the control to 75% hypotonic saline. The time windows used for the recovery period varied from 30 to 45 min. Values in this table were averaged from the average values calculated from eight axons. One of the eight preparations used sucrose substitution to generate hypotonic saline, two preparations used mannitol substitution and the remaining five used distilled water dilution.

* Subthreshold focused ultrasound−evoked depolarization responses only.

† Frequency was normalized to the maximum of 1, when ultrasound evoked responses in every trial.

‡ Boldface *p* values indicate statistically significant differences.

FUS-Specific membrane conductance g_{US} and nanopore hypothesis

As reviewed in the Introduction, application of FUS to an axonal membrane leads to an increase in membrane conductance (g_{US}) which underlies FUSD (Lin et al. 2019). Biophysical properties of g_{US}, namely, non-selective permeability and long duration, together with pharmacological properties, namely, absence of sensitivity to voltage-gated channel blockers, of FUSD led to the hypothesis that g_{US} may be mediated by nanopores formed in axonal membrane. In molecular dynamic simulations, similar lipid channels have been suggested to occur under electroporation and strong mechanical stretch (Tieleman et al. 2003; Leontiadou et al. 2004; Hu et al. 2005; Böckmann et al. 2008; Krasovitski et al. 2011). Furthermore, low-intensity FUS may also cause pore formation at the membrane protein−lipid interface (Babakhanian et al. 2018). Therefore, data presented here correspond well with characterizations based on quantitative simulations at the atomic level.

A schematic of nanopore formation in the context of stretched membrane is provided in Figure 5 to help interpret the results reported in this article. FUS-Mediated mechanical disturbance was assumed to disrupt lipid organization of axonal membrane, which leads to the opening of hydrophilic pores. The mechanical disturbance could cause lipid molecules to transition through a series of intermediate states (states 1 and 2) before settling in a relatively stable state (state 3) where the hydrophilic pores are well formed. These transitions could also be presented as a series of energy levels associated with the re-organization of the phospholipids (inset). According to molecular dynamic simulations, the stability of nanopores is influenced by the balance between membrane surface tension and line tension of open pores (Leontiadou et al. 2007). The line tension, in turn, is influenced by the organization of lipid tails as well as electrostatic interactions among ions, water molecules and charged head groups of lipid molecules around an open pore. It is therefore reasonable to anticipate that increases in membrane tension resulting from lowered osmotic pressure could enhance the probability of nanopore formation by way of decreasing the energy barriers between states and making transitions between states faster (*red potential levels* in the Fig. 5, inset). The increase in the probability of nanopore formation may underlie the increase in FUSD amplitude and frequency of occurrence, while the faster forward transitions could explain the reduction in FUSD delay. The reduction in FUSD duration could also be explained by the decreased energy difference between states 2 and 3 (Fig. 5, inset) such that the close rate of the open pores is increased in hypotonic saline.

Potential roles of radiation forces in FUSD

The design of experiments presented in this article was not intended to distinguish different US-generated physical processes underlying FUSD, such as forces generated by streaming, cavitation or radiation. However, the preparation used here, being a neuromuscular junction, could provide insights into potential contributions of radiation forces. We have examined and could not detect movement of the motor axons under a 60 × water immersion lens during FUS application, with the FUS transducer positioned below the preparation (unpublished data). Displacement in the range of ~1 μm should be visible under the 60 × lens. Furthermore, being a neuromuscular preparation, strong stimulation of the motor axons triggers muscle contractions, which also move the motor axons attached to it. In neurophysiological studies, recordings from muscle fibers and axons under the condition of mild contraction (≈100 μm in displacement) revealed small changes in membrane potential only during movement and were not stochastic. In contrast, FUSD was stochastic and had a duration of seconds in response to millisecond US tone bursts. Finally, we penetrated the axons with two electrodes routinely. The process of penetration invariably moved and deformed

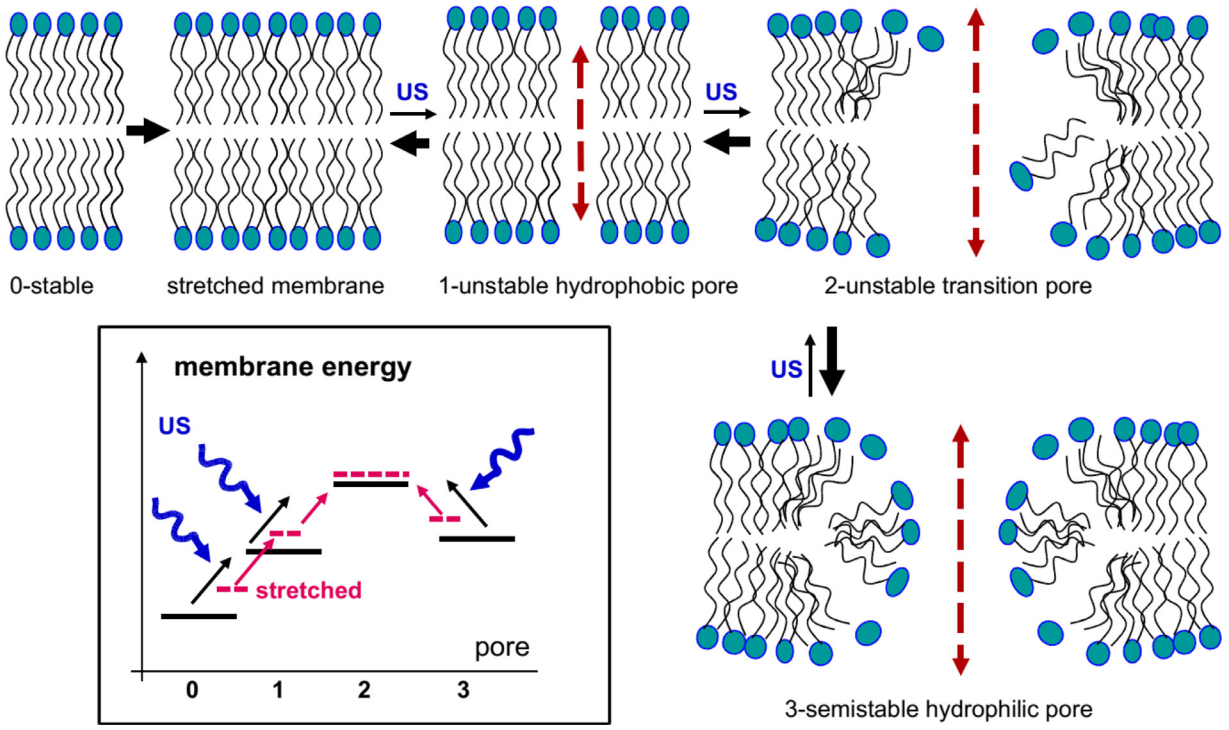

Fig. 5. Illustration of how osmotic stretching of the lipid membrane would affect the hypothetical lipid membrane energy levels, and state transitions caused by US, in comparison to control (= non-stretched) membrane. These changes may explain the observed effects of hypotonic saline on g_{US} opening and closing probabilities. Hypotonic solution stretches the membrane, that is, loosens the dense packing of the lipid bilayer (from 0-stable to stretched membrane); the increase in surface area corresponds to an increase in the membrane energy level (inset: *red* level vs. *black* level 0). From this stretched state, the opening of hydrophobic pores and transition pores requires less absorption of energy than in control (inset: *red uphill arrows* vs. *black uphill arrows* $0 \rightarrow 1 \rightarrow 2$, respectively), so that the probability of transition in response to absorption of US energy is increased. Similarly, the probability of the first step of stable nanopore closing is increased because of a decreased energy gap (inset: $3 \rightarrow 2$ *uphill red arrow* vs. *black arrow*, respectively). This change would reduce the mean open time of semi-stable hydrophobic pores 3 and, thus, the duration of g_{US}. US = ultrasound.

axonal membrane. During the penetration of the second electrode, the first electrode, which was intracellular already, detected only small changes in membrane potential roughly coinciding with, but never outlasting, the movement of the second electrode.

In summary, although radiation force may be important in certain preparations and experimental configurations, we believe that movement of the membrane caused by radiation forces is unlikely to be the cause of FUSD at the crayfish neuromuscular preparation. Radiational forces in the megahertz frequency range, however, may be altering the structure of the axonal membrane at a spatial scale <1 μm that cannot be easily observed under an optical microscope. This possibility would require a separate experimental approach to resolve.

Additional effects of hypotonic saline on motor axon

We believe the membrane depolarization produced by FUS (FUSD) is a general phenomenon applicable to all neurons as the structure and physical properties of membrane lipid bilayers are conserved across the evolutionary scale. However, we observed additional effects that may be cell type specific.

1 Effects of the osmolarity manipulation on axon morphology. The hypotonic saline had small effects on the crayfish motor axon morphology. When motor axon diameter was monitored with imaging, following fluorescence dye injection, no consistent increase in axonal diameter was detected (n = 4) in hypotonic saline (data not shown). Previous electron microscopic studies had indicated that the crayfish motor axons are encased in glia cells and extracellular matrix (Atwood and Morin 1970; Smith 1983). The latter could serve as a "brace" that prevents excessive swelling and rupture. In support of this unique resilience of the motor axon, the same hypotonic saline applied to the crayfish giant axons, in the central nervous system, caused measurable swelling (Yu et al., unpublished data). Furthermore, the crayfish giant axons exhibited reduced AP amplitude and hyperpolarization of RMP in hypotonic saline while none of

these parameters of motor axons was changed by low osmolarity. Therefore, the "resilience" of the motor axons in hypotonic saline may be uniquely relevant to peripheral neural tissues. The freshwater environment for crayfish means that any injury to the exoskeleton may result in a significant reduction in osmolarity locally. An extensive extracellular matrix that could contain excessive swelling of the axon may be part of the reason that swelling in motor axons was difficult to resolve microscopically in hypotonic saline. Results reported here may be applicable to vertebrate peripheral nerve tissues where axons typically are surrounded by a protective sheath such as perineurium and epineurium.

2 Time-dependent variation in FUSD parameters in hypotonic saline. The parameters of FUSD exhibited consistent changes that correlated with reduced osmolarity with a 15-min time window. However, the changes did not remain steady over the period of 45 min in hypotonic saline. Specifically, FUSD amplitude exhibited a large fluctuation within the 45-min period in hypotonic saline while FUSD duration gradually declined in the same period. As a result, averaged over a period of 45 min, FUSD amplitude in hypotonic saline was no longer statistically different from that in control saline while the duration became significantly shorter in low osmolarity. Changes in FUSD parameters were not reversed within the duration of our study ~30 min after the osmolarity was returned to the control saline.

This complexity may be due not only to the unique morphology of the extracellular matrix surrounding the crayfish motor axon, but also to cellular adaptation. Studies of membrane mechanics in other preparations provide clues to possible explanations. When a laser tweezer was used to stretch membrane and monitor the membrane tension of rat basophilic leukemia cells, it was found that the cells adapted to the tweezer stretching by inserting membrane over a period of 20 min (Dai and Sheetz 1995; Dai et al. 1997). Furthermore, plasma membrane and its linkage to submembranous cytoskeleton have been reported to change as the osmolarity of the bathing saline is altered (Morris and Homann 2001). The processes of insertion and retrieval of cell membrane, as well as disrupted linkage between membrane and submembranous cytoskeleton, could all take time to develop and recover. These cellular processes are relatively slow and could be the cause of delayed reduction of Dur_{50} (Fig. 4D) and recovery in FUSD amplitude (Fig. 4A), as well as the absence of recovery of all parameters after switching back to control saline (Table 1). Although amplitude, onset delay, frequency of occurrence and duration were used to characterize FUSD, these parameters may differentially be controlled by different cellular processes under stresses introduced by changing osmolarity. Therefore, although FUS may create nanopores in a lipid bilayer, the abilities of cells to add and retrieve membrane as well as break or form linkages between membrane lipid and molecules inside or outside of the membrane may all influence the formation and duration of nanopores.

Potential applications to human

We believe our finding on g_{US} from crayfish motor axons should be applicable to other preparations including neurons in the human brain, because the basic membrane structure and physiological properties are conserved across an evolutionary scale. Although we use 2-MHz FUS while 400- to 700-kHz US is typically used for humans, FUS across the entire range of the frequencies, from 0.4 to 2 MHz, should be capable of altering the lateral interactions between lipid molecules in neuronal membrane of the human central and peripheral nervous systems. In addition, the FUS pressure in this study is significantly below the FDA safety limit. Thus, the experimental regimen reported here should be safe for future tests in human applications.

In the long run, this study could be expanded to studies using mammalian brains where osmotic pressure is reduced under clinically relevant situations, such as during traumatic brain injuries or controlled reductions of osmolarity in circulating blood or cerebrospinal fluid. Furthermore, given the complexity of neuronal morphology, changes in US sensitivities of different neuronal compartments—such as soma, dendrites, axons and synaptic terminals—under low osmolarity should be evaluated in greater detail to fully understand the potentials of US neuromodulation.

CONCLUSIONS

Focused US-evoked membrane depolarization can be modulated by the osmolarity of the physiological saline surrounding the cell. Reduced osmolarity of the saline bathing the crayfish motor axon increased the amplitude, reduced the onset latency and increased the frequency of occurrence of FUSD immediately after osmolarity was lowered. The results support our hypothesis that FUSD may be generated by non-selective FUS-specific lipid ion channels whose activities are influenced by lateral surface tension in the membrane.

Acknowledgments—This work was Funded by National Science Foundation Grant 1707865 (Y.O., primary investigator; J.W.L., co-primary investigator).

REFERENCES

Atwood H. Parallel 'phasic' and 'tonic' motor systems of the crayfish abdomen. J Exp Biol 2008;211:2193–2195.

Atwood HL, Morin WA. Neuromuscular and axoaxonal synapses of the crayish opener muscle. J Ultrastruct Res 1970;32:351–369.

Babakhanian M, Yang L, Nowroozi B, Saddik G, Boodaghians L, Blount PAO, Grundfest W. Effects of low intensity focused ultrasound on liposomes containing channel proteins. Sci Rep 2018;8:17250.

Blackmore J, Shrivastava S, Sallet J, Butler CR, Cleveland RO. Ultrasound neuromodulation: A Review of results, mechanisms and safety. Ultrasound Med Biol 2019;45:1509–1536.

Böckmann RA, de Groot BL, Kakorin S, Neumann E, Grubmüller H. Kinetics, statistics, and energetics of lipid membrane electroporation studied by molecular dynamics simulations. Biophys J 2008;95:1837–1850.

Clement GT, Hynynen K. A non-invasive method for focusing ultrasound through the human skull. Phys Med Biol 2002;47:1219–1236.

Dai J, Sheetz MP. Mechanical properties of neuronal growth cone membranes studied by tether formation with laser optical tweezers. Biophys J 1995;68:988–996.

Dai J, Ting-Beall HP, Sheetz MP. The secretion-coupled endocytosis correlates with membrane tension changes in RBL 2H3 cells. J Gen Physiol 1997;110:1–10.

Delaney KR, Zucker RS, Tank DW. Calcium in motor nerve terminals associated with posttetanic potentiation. J Neurosci 1989;9:3558–3567.

Feng B, Chen L, Ilham SJ. A review on ultrasonic neuromodulation of the peripheral nervous system: Enhanced or suppressed activities? Appl Sci (Basel) 2019;9:1637.

Heimburg T. Lipid ion channels. Biophys Chem 2010;150:2–22.

Hu Q, Joshi RP, Schoenbach KH. Simulations of nanopore formation and phosphatidylserine externalization in lipid membranes subjected to a high-intensity, ultrashort electric pulse. Phys Rev E Stat Nonlin Soft Matter Phys 2005;72 031902.

Krasovitski B, Frenkel V, Shoham S, Kimmel E. Intramembrane cavitation as a unifying mechanism for ultrasound-induced bioeffects. Proc Natl Acad Sci USA 2011;108:3258–3263.

Kubanek J, Shi J, Marsh J, Chen D, Deng C, Cui J. Ultrasound modulates ion channel currents. Sci Rep 2016;6:24170.

Kubanek J, Shukla P, Das A, Baccus SA, Goodman MB. Ultrasound elicits behavioral responses through mechanical effects on neurons and ion channels in a simple nervous system. J Neurosci 2018;38:3081–3091.

Leontiadou H, Mark AE, Marrink SJ. Molecular dynamics simulations of hydrophilic pores in lipid bilayers. Biophys J 2004;86:2156–2164.

Leontiadou H, Mark AE, Marrink SJ. Ion transport across transmembrane pores. Biophys J 2007;92:4209–4215.

Lin JW. Spatial variation in membrane excitability modulated by 4-AP-sensitive K^+ channels in the axons of the crayfish neuromuscular junction. J Neurophysiol 2012;107:2692–2702.

Lin JW. Spatial gradient in TTX sensitivity of axons at the crayfish opener neuromuscular junction. J Neurophysiol 2013;109:162–170.

Lin JW, Yu F, Muller WS, Ehnholm G, Okada Y. Focused ultrasound transiently increases membrane conductance in isolated crayfish axon. J Neurophysiol 2019;121:480–489.

Miller DL. Safety assurance in obstetrical ultrasound. Semin Ultrasound CT MR 2008;29:156–164.

Morris CE, Homann U. Cell surface area regulation and membrane tension. J Membr Biol 2001;179:79–102.

Morris CE, Juranka PF. Nav channel mechanosensitivity: Activation and inactivation accelerate reversibly with stretch. Biophys J 2007;93:822–833.

Mulkey RM, Zucker RS. Calcium released by photolysis of DM-nitrophen triggers transmitter release at the crayfish neuromuscular junction. J Physiol 1993;462:243–260.

Naor O, Krupa S, Shoham S. Ultrasonic neuromodulation. J Neural Eng 2016;13 031003.

Prieto ML, Omer O, Khuri-Yakub BT, Maduke MC. Dynamic response of model lipid membranes to ultrasonic radiation force. PLoS One 2013;8:e77115.

Smith DO. Extracellular potassium levels and axon excitability during repetitive action potentials in crayfish. J Physiol 1983;336:143–157.

Tieleman DP, Leontiadou H, Mark AE, Marrink SJ. Simulation of pore formation in lipid bilayers by mechanical stress and electric fields. J Am Chem Soc 2003;125:6382–6383.

Tufail Y, Matyushov A, Baldwin N, Tauchmann ML, Georges J, Yoshihiro A, Tillery SI, Tyler WJ. Transcranial pulsed ultrasound stimulates intact brain circuits. Neuron 2010;66:681–694.

Tyler WJ, Tufail Y, Finsterwald M, Tauchmann ML, Olson EJ, Majestic C. Remote excitation of neuronal circuits using low-intensity, low-frequency ultrasound. PLoS One 2008;3:e3511.

Tyler WJ, Tufail Y, Pati S. Pain: Noninvasive functional neurosurgery using ultrasound. Nat Rev Neurol 2010;6:13–14.

Vyshedskiy A, Lin JW. Study of the inhibitor of the crayfish neuromuscular junction by presynaptic voltage control. J Neurophysiol 1997;77:103–115.

Wright SN, Brodwick MS, Bittner GD. Presynaptic calcium currents at voltage-clamped excitor and inhibitor nerve terminals of crayfish. J Physiol 1996;496(Pt 2):347–361.

Wu J, Lewis AH, Grandl J. Touch, tension, and transduction—The function and regulation of piezo ion channels. Trends Biochem Sci 2017;42:57–71.

Zhang T, Pan N, Wang Y, Liu C, Hu S. Transcranial focused ultrasound neuromodulation: A review of the excitatory and inhibitory effects on brain activity in human and animals. Front Hum Neurosci 2021;15 749162.

Zhu X, Lin JW, Sander MY. Infrared inhibition and waveform modulation of action potentials in the crayfish motor axon. Biomed Opt Express 2019;10:6580–6594.